Acta Cryst. (1995). B**51**, 48–54

X-ray Study of and Structural Approach to the Incommensurate Perovskite Pb_2CoWO_6

BY MICHEL BONIN, WŁODEK PACIOREK, KURT J. SCHENK AND GERVAIS CHAPUIS

Institut de Cristallographie, Université de Lausanne, BSP Dorigny, CH-1015 Lausanne, Switzerland

(*Received* 21 *April* 1994; *accepted* 28 *September* 1994)

Abstract

Pb_2CoWO_6 in its incommensurate phase ($230 \leq T \leq 300$ K) invariably exhibits orientational domains. Such a polydomain state has been investigated by means of X-ray diffraction at 283 K. Assuming the modulation to be one-dimensional, we have identified the orientations of four domains. In view of the pseudosymmetry of this phase, many refinements of a purely displacive modulation had to be performed in order to establish the best suited unit cell and superspace group. Two major categories of candidates have arisen from this approach. (i) In a centered monoclinic or triclinic cell, there were clear indications of disorder in the structure, but owing to numerical instabilities, it was very difficult to decide whether this phenomenon was due to an occupational modulation or to a more complex domain structure (overlapping satellites, presence of antiphase domain boundaries *etc.*). (ii) In a primitive monoclinic cell model, a purely displacive modulation was conclusive. In each category, the major feature is an antiparallel shift of the Pb atoms. The main component of this shift involves a rotation and/or deformation of the oxygen octahedra. The structure of Pb_2CoWO_6 may be described to a good approximation as displacively modulated, but occupational modulation and coherent domains will also have to be added to the model in order to reach an even more satisfactory picture of this elusive phase.

Introduction

The complex perovskite Pb_2CoWO_6 (PCW) exhibits some fascinating features that make it an ideal study ground for both material science and the theory of phase transitions. Its utility is, however, severely hampered by several growth sectors (Brixel, Boutellier & Schmid, 1987) and the existence of microdomains in most of its phases. These domains almost entirely thwart any kind of physical measurement and, not surprisingly, rather diverging opinions may be retrieved from the literature. The structure of PCW is presented in Fig. 1 and its phase diagram in Table 1.

The unit cell, $a_c = 8.013$ Å, and space group, $Fm\bar{3}m$, of phase I (above 300 K) are certainly widely accepted, and even the structure offers little reason for doubt. Co and W atoms are perfectly ordered, whereas Pb and O atoms occupy the disordered positions (Baldinozzi, Sciau & Lapasset, 1992) known from other perovskites.

There exists some consensus regarding the crystal system of phase II (300–230 K). Optical crystallography (Brixel, Werk, Fischer, Bührer, Rivera, Tissot & Schmid, 1985), X-ray powder diffraction (Kim, Lee & Choo, 1992) and especially the powerful electron-diffraction study by Sciau, Krusche, Buffat & Schmid (1990) conclude phase II to be monoclinic with the unique axis lying along one of the cubic [011] axes. The metric is pseudotetragonal, but more precise experiments suspect one of the angles to be slightly different to 90°. Phase II is a multidomain state, as shown by Sciau *et al.* (1990) and Randall, Markgraf, Bhalla & Baba-Kishi (1989). The unit cell and space group are strongly author dependent. This divergence is not surprising for it is clear that normal X-ray diffraction cannot yield the correct unit cell because of the overlapping of reflections from different domains, and powder diffraction can overlook doubling of the cell too easily. Recently, however, in a careful high-resolution X-ray investigation Sciau, Calvarin, Sun

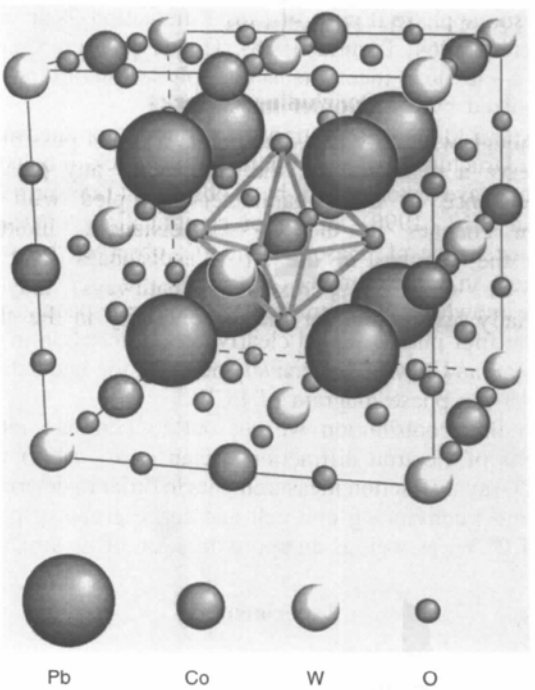

Fig. 1. View of the double perovskite Pb_2CoWO_6.

Table 1. *Phase diagram of* Pb_2CoWO_6

Question marks indicate unconfirmed or unknown properties.

	First order 300 K		First order 230 K	9 K
	Phase I	Phase II	Phase III	Phase IV
	Cubic	Monoclinic (Inc.)	Orthorhombic	Orthorhombic
	Fm3m (Z = 4)	*2/m* (Z = ?)	$P2_1cn$ (Z = 4)	?
	Paraelectric	Antiferroelectric(?)	Ferroelectric(?)	?
	Paraelastic	Ferroelastic	Ferroelastic	?
	Paramagnetic	Paramagnetic	Paramagnetic	Ferromagnetic

& Schmid (1992) have made a strong case for a cell: $\mathbf{a}_m = \mathbf{a}_c$, $\mathbf{b}_m = \frac{1}{2}(\mathbf{b}_c + \mathbf{c}_c)$, $\mathbf{c}_m = \frac{1}{2}(-\mathbf{b}_c + \mathbf{c}_c)$.

Of phase III (below 230 K), only the unit cell $\mathbf{a}_o = \mathbf{a}_c$, $\mathbf{b}_o = \frac{1}{2}(\mathbf{b}_c + \mathbf{c}_c)$, $\mathbf{c}_o = -\mathbf{b}_c + \mathbf{c}_c$ (Bührer, Rüdlinger, Maaroufi, Toledano, Schmid, Brixel & Sciau, 1989) and the space group, $P2_1cn$ or *Pmcn*, (Baldinozzi, Sciau & Buffat, 1993) are known. The orientations of $\mathbf{b}_o$ and $\mathbf{c}_o$, however, with respect to the cubic axes are not at all clear. The former space group should be favored since it allows an ordered ferroelectric configuration. The rotation of the oxygen octahedra about $\mathbf{a}_o = \mathbf{a}_c$, found in the isomorphous Pb_2MgWO_6 by Baldinozzi *et al.* (1993), might turn out to be valid for PCW as well. In any case, it has already been postulated by Aleksandrov & Misyul (1981) in a theoretical analysis of the possible low-temperature phases in double perovskites.

Very little is known about phase IV. It has been mentioned by Kizhaev & Bokov (1966) and Brixel *et al.* (1985), and its symmetry is conjectured to be orthogonal. Indeed, the III→IV transition at ~9 K seems to be of magnetic or magnetic–structural origin.

At ~300 K, phase I is transformed into the incommensurate phase II *via* a first-order transition (Filip'ev & Fesenko, 1964; Tamura, 1978). This is quite unexpected for a classical incommensurate phase should not be stabilized by a first-order transition.

At ~230 K, phase II transforms into a commensurate superstructure, phase III, but the typical lock-in behavior of the wavevector has not been observed (Tamura, 1978; Sciau *et al.*, 1990). A further complication consists of a coexistence of phases II and III, observed by some authors in some samples.

A knowledge of even the unit cells and space groups of the four phases would clearly benefit research in this system, and it would decisively advance the understanding of the phase diagram of PCW.

In this contribution we set out to combine recent results of electron diffraction (Sciau *et al.*, 1990) with our X-ray diffraction measurements in order to determine the most convincing unit cell and space group of phase II of PCW, as well as an approximation of its structure.

Experimental

Selection of the sample

The samples of PCW used in this study have been grown using a flux of PbO (Sun, Bouteiller, Sciau, Burkhardt, Rodriguez & Schmid, 1991). Two types of specimens were tested for X-ray analysis: polished thin sections prepared for optical microscopy of ferroelastic domains and unpolished samples. Better X-ray results were obtained from the latter. Specimens with thickness $10 \le d \le 100\,\mu m$, which permitted the observation of extinction under crossed Nicols for at least one orientation, were selected.

The chosen sample was first examined on a precession chamber by recording several reciprocal layers. The satellite reflections could be clearly identified, and no splitting of main reflections was detected. The absence of commensurate superstructure reflections was also verified (by visual inspection). The principal reflections could be indexed according to the cubic *F*-centered cell of phase I (Fig. 1). Satellite reflections appeared in the vicinity of the systematically absent reflections (*hkl*) = (*eoo*) or (*hkl*) = (*oee*), the latter ones being very weak. All satellites could be expressed in terms of the four vectors

$$\mathbf{Q}_1 = \pm(q_{c1}, q_{c2}, q_{c3}),$$

$$\mathbf{Q}_2 = \pm(-q_{c1}, q_{c2}, q_{c3}),$$

$$\mathbf{Q}_3 = \pm(q_{c1}, q_{c2}, -q_{c3}),$$

$$\mathbf{Q}_4 = \pm(-q_{c1}, q_{c2}, -q_{c3}),$$

with $q_{c1} \simeq \frac{1}{12}$ and $q_{c2} = q_{c3} \simeq \frac{1}{6}$.

Subscripts are used as follows: *c* cubic, *m* monoclinic and *o* orthorhombic.

Data collection

The sample was measured on an automatic diffractometer (CAD-4, Delft Instruments) at a temperature of 283 ± 1 K (Oxford Cryosystems). To minimize absorption, silver radiation was used (λ = 0.56087 Å). Intensities were recorded using the standard $\omega/2\theta$ technique. First, main reflections ($0 \le 2\theta \le 60°$) were collected, then satellites ($0 \le 2\theta \le 42°$). For each reflection $\mathbf{H} = (hkl)$, eight satellites were measured at $\mathbf{H} \pm \mathbf{Q}_i$ (i = 1,4). Absorption (Gaussian integration, based on morphology), Lorentz and polarization corrections were applied to intensities. The stability of the experimental setting was monitored by periodically measuring standard reflections including main and satellite intensities (Table 2).

Unit cell and superspace group

The lattice parameters of the pseudotetragonal cell, obtained from accurately centering 25 reflections, are presented in Table 2. The long-standing ambiguity regarding the type of modulation in PCW seems to have been resolved by Sciau *et al.* (1990). Indeed, these authors have shown that a monodomain of PCW exhibits a one-dimensional modulation. Our eight observed satellites must, therefore, be interpreted as

Table 2. *Crystal data and DC parameters for* Pb_2CoWO_6 *at* 283 K

Temperature (K)	283.0 (5)
a (Å)	7.964 (2)
b (Å)	8.021 (2)
c (Å)	8.023 (2)
α (°)	89.90 (2)
β (°)	90.00 (2)
γ (°)	90.00 (2)
V (Å^3)	512.5 (2)
Z	4
M_r	753.2
λ (Å)	0.56086
Scan width	0.60 + 0.45tanθ (main)
	0.70 + 0.45tanθ (satellites)
Scan speed (° min^{-1})	0.12–6.71
μ(Ag $K\alpha$) (mm^{-1})	49.50
T_{min}/T_{max}	0.037/0.369
D_x (g cm^{-3})	9.77
$F(000)$	1252
Modulation vector	$\mathbf{q}$ = 0.081 (5)**a*** + 0.164 (5)**b** + 0.164 (5)**c***
(m = 0) $14 \le h \le -1$	7080 main reflections
$-14 \le k \le 14$	
$-14 \le l \le 14$	
($\|m\|$ = 1) $0 \le h \le -10$	3180 satellite reflections
$-9 \le k \le 9$	
$-9 \le l \le 9$	
Loss of standard intensities	<1% for main reflections (850h)
	<1% for satellites (220h)
Fluctuations	$\|I_s - \bar{I}_s\| < 4$ e.s.d. ($\bar{I}_s$)

a superposition of four orientational domains. For a single-domain orientation, the modulation vector can be expressed as $\mathbf{q}_c \simeq \pm(\frac{1}{12},\frac{1}{6},\frac{1}{6})$. The remaining orientations can be obtained, *e.g.* by rotations about the pseudotetragonal axis $\mathbf{a}_c^*$ by ±90 and ±180° (Fig. 2).

The data collection did confirm that the satellites tend to cluster around the systematically absent reflections of the F-centered cell with parity classes (*eoo*) and (*oee*). The lattice centering is thus maintained and the symmetry of the incommensurate phase can be described in terms of a centered cell assuming an adequate choice of the irrational part of the modulation wavevector. One such possibility is an I-centered Bravais lattice in the cell $\mathbf{a_m} = \mathbf{a_c}$, $\mathbf{b_m} = \frac{1}{2}(\mathbf{b_c} + \mathbf{c_c})$, $\mathbf{c_m} = \frac{1}{2}(-\mathbf{b_c} + \mathbf{c_c})$ [Fig. 3(*a*)]. In these axes, the modulation vectors corresponding to the identity domain have the form $\mathbf{q}_{m1} \simeq \pm(\frac{11}{12},0,\frac{1}{6})$ or $\mathbf{q}_{m2} \simeq \pm(\frac{1}{12},0,\frac{5}{6})$, and the satellite reflections lie in the reciprocal plane perpendicular to the monoclinic axis [Fig. 3(*b*)]. Accordingly, the Bravais class in superspace (de Wolff, Janssen & Janner, 1981) is

$$P^{I\,2/m}_{1\;1}.$$

The 3180 satellite reflections can be classified in four sets D_1, D_2, D_3 and D_4, corresponding to $\mathbf{Q}_i$ (i = 1,4). For each set, the internal agreement for data larger than 3σ (2127 reflections) in the Laue symmetry $2/m$ is presented in Table 3. The agreement being reasonable in each of the domains, the solution of the incommensurate phase has been undertaken with the complete set of measurements. This method has the advantage of removing the ambiguities on the exact intensities of the main reflections (Jameson, 1982).

The systematic absences of the 2644 satellite reflections larger or equal to zero were analyzed. The four classes of satellite reflections seem to comply (Table 4) with the special reflection condition $m = 2n$ for $h0lm$ reflections (monoclinic axis **b***). Within the 3σ criterion we can propose the following superspace group (de Wolff *et al.*, 1981) or any of its subgroups

$$P^{I\,2/m}_{1\;1}.$$

From the 2127 reflections larger than 3σ, 40 reflections were rejected on the basis of their profile.

Structure refinements

Some refinements, using the two modulation vectors $\mathbf{q}_{m1}$ and $\mathbf{q}_{m2}$, were carried out in the I-centered cell $\mathbf{a_m} = \mathbf{a_c}$, $\mathbf{b_m} = \frac{1}{2}(\mathbf{b_c} + \mathbf{c_c})$, $\mathbf{c_m} = \frac{1}{2}(-\mathbf{b_c} + \mathbf{c_c})$, while others

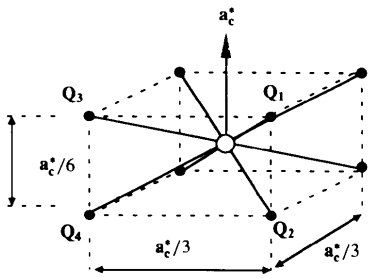

Fig. 2. Illustration of twin components and satellite (full circles) configuration around a forbidden main reflection (open circle). Each domain D_i (i = 1,4) corresponds to a vector $\mathbf{Q}_i$ (i = 1,4), as defined in *Selection of the sample* in the *Experimental* section.

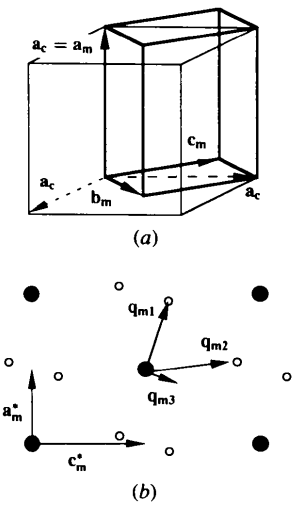

Fig. 3. (*a*) Monoclinic basis vectors (bold) described in terms of the cubic F-centered cell. (*b*) (h,2n,l)-type layers in the monoclinic indexation and different choices of the modulation vectors $\mathbf{q}$. (Main reflections, full circles; satellite reflections, open circles.) The vector $\mathbf{q}_{m3}$ corresponds to the vector $\mathbf{q}_c$ which was used for the collection of the data reported in Table 2.

Table 3. *Internal agreement factors R_{int} for the intensities of equivalent satellite reflections in Laue symmetry 2/m for each of the four classes D_1, D_2, D_3, D_4*

$$R_{int} = \{[\sum_i N_i \sum_s w_{s,i}(\bar{F}_i - F_{s,i})^2]/[\sum_i (N_i - 1)\sum_s w_{s,i}F_{s,i}^2]\}^{1/2},$$

where the summation s involves the N_i symmetry-equivalent reflections with weight w_i and i the independent group of reflections (Blessing, 1987).

Domain	Reflections $I > 3\sigma(I)$	R_{int}	Unique reflections
D_1	589	0.096	249
D_2	580	0.085	246
D_3	358	0.153	169
D_4	600	0.100	249

Table 4. *Systematic absences corresponding to superspace-group operation m(s) for each of the four satellite classes D_1, D_2, D_3 and D_4*

Domain	Reflections	*h0lm* type	*h0lm* type $I < 3(I)$
D_1	682	25	25
D_2	694	26	26
		hk0m type	*hk0m* type $I < 3\sigma(I)$
D_3	569	32	32
D_4	699	26	26

were based on the corresponding primitive cell and $\mathbf{q}_{m1}$. Further refinements, considering $\mathbf{q}_{m4} \simeq \pm (\frac{11}{12},0,\frac{1}{3})$, were also undertaken in the primitive cell $\mathbf{a_m} = \mathbf{a_c}$, $\mathbf{b_m} = \frac{1}{2}(\mathbf{b_c} + \mathbf{c_c})$, $\mathbf{c_m} = (-\mathbf{b_c} + \mathbf{c_c})$.

Treatment of domains

The program prepared for our refinements is an extension of Paciorek's (1991) *MSR* program. New features have been added for refining data from multiple macroscopic domains, and for treating partially overlapping main reflections correctly.

In this formalism, point-group operations R_i are derived that link a satellite reflection from domain i to the corresponding satellite of a reference domain (associated with the identity operation). These symmetry operations are then used to compute the structure factor of the main reflections (that contain contributions from all domains) according to

$$F_c^2 = \sum_{i=1}^{n-1} \alpha_i F_i^2 + \left(1 - \sum_{i=1}^{n-1} \alpha_i\right) F_n^2.$$

In this expression α_i is the volume fraction occupied by the ith domain (α_i may be determined from the satellite intensities), n represents the total number of domains of which $n-1$ are independent ($\sum_{i=1}^{n} \alpha_i = 1$), and $F_i(\mathbf{H}) = F_n(R_i^t\mathbf{H})$ (F_n is the structure factor corresponding to the identity operation (domain) and R_i the symmetry operation generating the ith domain).

The expression for the atomic coordinates is given by

$$x_i^\mu(\bar{x}_4) = \bar{x}_i^\mu + u_i^\mu(\bar{x}_4),$$

where $\bar{x}_4 = \mathbf{q}.\mathbf{x} + t$ and u_i^μ is the modulation function for the ith coordinate of the μth atom. The programme refines the coefficients of the expansion

$$u_i^\mu(\bar{x}_4) = \sum_{n>0} (a_{i,n}^\mu c_n + b_{i,n}^\mu s_n),$$

with $c_n = \cos(2\pi n\bar{x}_4)$ and $s_n = \sin(2\pi n\bar{x}_4)$.

Results

Since only first-order satellites could be observed, and because of the presence of several orientational domains it appeared necessary to confirm our tentative reflection condition ($m = 2n$ for *h0lm*) by preliminary refinements. These unambiguously yielded the existence of the superspace symmetry operation $m(s)$ corresponding to a mirror plane associated with a phase shift of $\frac{1}{2}$ along t (Tables 5*a* and 5*b*). If this structure contains a mirror operation, it can only be of the type $m(s)$. The twin operations relating the four domains were identified by a refinement in *I*2/*m* and using the modulation vectors $\mathbf{q}_{m1} \simeq \pm (\frac{11}{12},0,\frac{1}{6})$ or $\mathbf{q}_{m2} \simeq \pm (\frac{1}{12},0,\frac{5}{6})$. The respective population parameters associated with the four domains rotated by π, $\pi/2$ and $-\pi/2$ (operations 2,3,4 in Tables 5*a* and 5*b*) correspond to the best agreement.*

We emphasize that the proposed domain structure leaves the direction $[100]_c$ invariant and is thus compatible with our refined lattice parameters and those obtained from powder diffraction. Indeed, a symmetry operation requesting permutations of the type $[100]_c/[010]_c$ or $[100]_c/[001]_c$ would yield for $[100]_c$ an average value closer to $[010]_c$ or $[001]_c$.

The refinement in the *I*-centered cell $\mathbf{a_m} = \mathbf{a_c}$, $\mathbf{b_m} = \frac{1}{2}(\mathbf{b_c} + \mathbf{c_c})$, $\mathbf{c_m} = \frac{1}{2}(-\mathbf{b_c} + \mathbf{c_c})$, in $2/m(\bar{1},s)$, modulation vector $\mathbf{q}_{m1} \simeq \pm (\frac{11}{12},0,\frac{1}{6})$ and using anisotropic displacement parameters (ADP's), converged rapidly. This model confirms the displacive character of the modulation, which can be interpreted as a transverse displacement with a polarization normal to the monoclinic plane. It is, however, necessary to mention that the corresponding ADP, β_{33}, is huge (Table 6*a*). Fig. 4 reveals some structural characteristics obtained in $I2/m(\bar{1},s)$ with $\mathbf{q}_{m1}$. Various attempts to release the symmetry constraints on the atoms did not improve the ADP's. The only modification which seems to be able to influence these parameters is a reduction to triclinic symmetry (Table 6*b*) or a change to a primitive lattice (Table 7). Additional refinements in the monoclinic *I*-centered cell and the alternative choice of the modulation vector $\mathbf{q}_{m2} \simeq \pm (\frac{1}{12},0,\frac{5}{6})$ have been carried out. If the nature of the mirror plane is confirmed, the convergence is, however, very slow, especially for satellites. The displacement parameters become nonpositive definite. This model can thus be discarded. The results presented in Table 8 have been obtained in $I2/m(\bar{1},s)$.

* A list of the structure factors has been deposited with the IUCr (Reference: JS0003). Copies may be obtained through The Managing Editor, International Union of Crystallography, 5 Abbey Square, Chester CH1 2HU, England.

Table 5. *Results of a preliminary isotropic refinement in I2/m($\bar{1}$,1) and I2/m($\bar{1}$,s) for* $\mathbf{q}_{m1}$ *and* $\mathbf{q}_{m2}$

OSR is defined as the ratio $\sum F_c/\sum F_o$.

(*a*) $\mathbf{q}_{m1}$

		I2/m($\bar{1}$,s)	q = (11/12,0,1/6)		I2/m($\bar{1}$,1)	q = (11/12,0,1/6)	
Twin operation		V_{frac}				V_{frac}	
D_1		0.2759 (17)				0.2608 (90)	
D_2		0.3072 (11)				0.2732 (52)	
D_3		0.3563 (11)				0.3238 (55)	
D_4		0.0606 (56)				0.1421 (49)	
Layers	m = −1	m = 0	m = 1	m = −1	m = 0	m = 1	
No of reflections	1000	1606	1087	1000	1606	1087	
OSR	0.9701	1.0181	0.9554	0.6607	0.9833	0.6552	
R_w	0.1327	0.0650	0.1391	0.6642	0.1042	0.6324	
R	0.1192	0.0630	0.1307	0.6126	0.0924	0.5706	

(*b*) $\mathbf{q}_{m2}$

		I2/m($\bar{1}$,s)	q = (1/12,0,5/6)		I2/m($\bar{1}$,1)	q = (1/12,0,5/6)	
Twin operation		V_{frac}				V_{frac}	
D_1		0.2772 (29)				0.2547 (93)	
D_2		0.3144 (20)				0.2781 (55)	
D_3		0.0591 (94)				0.1245 (48)	
D_4		0.3492 (19)				0.3426 (58)	
Layers	m = −1	m = 0	m = 1	m = −1	m = 0	m = 1	
No of reflections	1087	1606	1000	1087	1606	1000	
OSR	0.9059	0.9940	0.9674	0.5565	1.0003	0.6158	
R_w	0.2120	0.1140	0.2185	0.6780	0.0924	0.6543	
R	0.1872	0.0801	0.1919	0.6133	0.0770	0.5997	

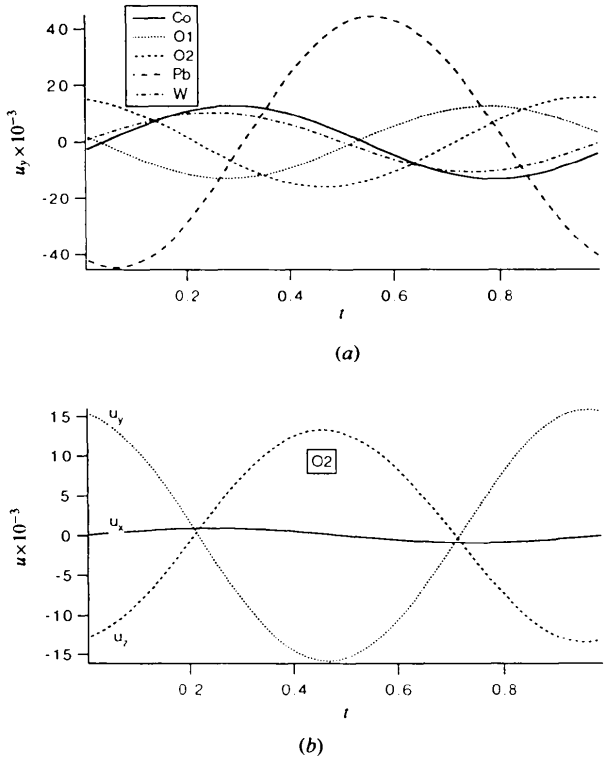

Fig. 4. Structural characteristics obtained using I2/m($\bar{1}$,s) and $\mathbf{q}_{m1}$. (*a*) Modulation displacements along *y* for all atoms and (*b*) modulation displacements for O2 in a general position.

The results obtained in the refinement of the model featuring $\mathbf{q}_{m1} \simeq \pm(\frac{11}{12},0,\frac{1}{6})$ and a primitive lattice indicate that the low-temperature cell $\mathbf{a_m} = \mathbf{a_c}$, $\mathbf{b_m} = \frac{1}{2}(\mathbf{b_c} + \mathbf{c_c})$, $\mathbf{c_m} = (-\mathbf{b_c} + \mathbf{c_c})$, found by Baldinozzi *et al.* (1993), might also be a plausible choice for the average cell of phase II. Such a model was, therefore, tested although the refinement had to be carried out with a subset of the necessary reflections. This refinement with superspace symmetry *Pm*(*s*) and $\mathbf{q}_{m4} \simeq \pm(\frac{11}{12},0,\frac{1}{3})$ converged remarkably well and gave excellent agreements (Table 9). The ADP's of the Pb atoms are more compatible with a displacive model. The structural characteristics of this refinement are presented in Fig. 5. From the variation of θ (Fig. 6) and a rigid-body approximation, it is possible to evaluate the maximum value of the rotation φ of the oxygen octahedra. This value of $\varphi_{max} = |\theta - \pi/2|/2 \simeq 7.5°$ is pleasingly close to the value refined by Baldinozzi *et al.* (1993) for the low-temperature phase of the isomorphous Pb_2MgWO_6.

Discussion

A series of refinements of the incommensurate phase of Pb_2CoWO_6 have been performed for the first time on a multidomain sample consisting of four orientational domains, the identity and three domains generated by rotation of 90, 180 and 270° about one of the cubic axes of phase I (*a* in Table 2). In the incommensurate phase and cubic setting, this axis is well differentiated from

Table 6. *Results of a refinement in I2/m(1̄,s) and in I1 for* $\mathbf{q}_{m1}$, *with ADP's for the* Pb *atoms*

The 32 refined parameters include scale factor, extinction and three twin-volume fractions. All the noncoordinate parameters absent in the table are constrained by symmetry to be equal to zero (Petříček & Coppens, 1988).

(*a*) *I*2/*m* (1̄,*s*)

Layers	All	*m* = −1	*m* = 0	*m* = 1
No. of reflections	3693	1000	1606	1087
OSR	0.9964	0.9977	1.0026	0.9693
R_w	0.0662	0.0946	0.0508	0.1053
R	0.0570	0.0792	0.0431	0.0958

Pb	x_1	0.24866 (7)	O1	x_1	0.2378 (6)
	x_2	0*		x_2	0*
	$a_{2,1}$	0.03052 (5)		$a_{2,1}$	0.0127 (9)
	$b_{2,1}$	−0.03345 (9)		$b_{2,1}$	−0.000 (1)
	x_3	0.49662 (8)		x_3	−0.0375 (9)
	β_{11}	0.00735 (3)		u	0.0146 (9)
	β_{22}	0.00378 (6)			
	β_{33}	0.01354 (7)	O2	x_1	0.0183 (5)
	β_{13}	0.00057 (7)		$a_{1,1}$	0.0001 (6)
				$b_{1,1}$	0.001 (1)
Co	x_1	1/2*		x_2	0.2347 (7)
	x_2	0*		$a_{2,1}$	0.0151 (6)
	x_3	0*		$b_{2,1}$	0.002 (1)
	$a_{2,1}$	−0.01378 (28)		x_3	0.2425 (7)
	u	0.00430 (11)		$a_{3,1}$	−0.0134 (6)
				$b_{3,1}$	−0.001 (1)
W	x_1	0*		u	0.0135 (5)
	x_2	0*			
	x_3	0*			
	$a_{2,1}$	0.01028 (9)			
	u	0.00682 (3)			

(*b*) *I*1

Layers	All	*m* = −1	*m* = 0	*m* = 1
No. of reflections	3693	1000	1606	1087
OSR	0.9985	1.0103	0.9990	0.9860
R_w	0.0656	0.0923	0.0540	0.0940
R	0.0574	0.0801	0.0457	0.0863

	Pb_1	Pb_2
x_1	0.25219 (11)	0.75087 (12)
$a_{1,1}$	0.00476 (15)	0.00517 (15)
$b_{1,1}$	0.01003 (14)	0.00975 (16)
x_2	0.00064 (12)	−0.00689 (12)
$a_{2,1}$	0.02826 (16)	−0.01728 (17)
$b_{2,1}$	−0.01828 (19)	0.01744 (19)
x_3	0.49721 (12)	0.49756 (13)
$a_{3,1}$	0.02451 (15)	0.02652 (16)
$b_{3,1}$	0.02118 (18)	0.02289 (19)
β_{11}	0.00523 (06)	0.00741 (08)
β_{22}	0.00695 (11)	0.01091 (15)
β_{33}	0.00832 (16)	0.00956 (19)
β_{12}	0.00200 (10)	−0.00284 (13)
β_{13}	−0.00214 (14)	−0.00506 (17)
β_{23}	−0.00370 (13)	0.00244 (18)

* Coordinates invariant due to special positions.

the other two. The indexation of the satellites (direction of the modulation) and the symmetry 2/*m*(1̄,*s*) or *m*(*s*) in superspace has been clearly established.

Our simplest model (closest to observations) is based on a monoclinic cell derived from the pseudotetragonal cell. In the *I*-centered cell $\mathbf{a_m} = \mathbf{a_c}$, $\mathbf{b_m} = \frac{1}{2}(\mathbf{b_c} + \mathbf{c_c})$, $\mathbf{c_m} = \frac{1}{2}(-\mathbf{b_c} + \mathbf{c_c})$, the refinements are very satisfactory, although some ADP's are too large.

Table 7. *Results of a refinement in Pm(s) for* $\mathbf{q}_{m1}$, *with ADP's for the* Pb *atoms*

Layers	All	*m* = −1	*m* = 0	*m* = 1
No. of reflections	3693	1000	1606	1087
OSR	0.9987	0.9932	1.0011	0.9936
R_w	0.0571	0.0895	0.0408	0.0923
R	0.0478	0.0758	0.0333	0.0836

	Pb_1	Pb_2	Pb_3	Pb_4
x_1	0.26156 (17)	0.74086 (17)	0.26219 (17)	0.74741 (17)
$a_{2,1}$	0.03514 (24)	0.03676 (30)	−0.02953 (32)	0.04487 (25)
$b_{2,1}$	−0.02729 (25)	0.02189 (27)	0.03638 (27)	0.00094 (26)
x_3	0.48030 (23)	0.49264 (26)	0.00418 (33)	0.01335 (22)
β_{11}	0.00452 (09)	0.00797 (16)	0.00387 (09)	0.00912 (16)
β_{22}	0.00283 (17)	0.00968 (34)	0.00524 (19)	0.00295 (26)
β_{33}	0.00740 (21)	0.01243 (28)	0.01419 (27)	0.00804 (25)
β_{13}	0.00111 (14)	−0.00320 (25)	0.00079 (21)	0.00244 (19)

Table 8. *Results of a refinement in I2/m(1̄,s) for* $\mathbf{q}_{m2}$, *with ADP's for the* Pb *atom*

Layers	All	*m* = −1	*m* = 0	*m* = 1
No. of reflections	3693	1087	1606	1000
OSR	0.9902	0.9495	1.0026	0.9779
R_w	0.0903	0.1570	0.0495	0.1668
R	0.0717	0.1346	0.0419	0.1402

	Pb
x_1	0.24871 (7)
$a_{2,1}$	0.03283 (9)
$b_{2,1}$	−0.03082 (6)
x_3	0.50030 (9)
β_{11}	0.00731 (3)
β_{22}	0.00400 (6)
β_{33}	0.01389 (8)
β_{13}	0.00016 (8)

The refinements in a primitive cell $\mathbf{a_m} = \mathbf{a_c}$, $\mathbf{b_m} = \frac{1}{2}(\mathbf{b_c} + \mathbf{c_c})$, $\mathbf{c_m} = (-\mathbf{b_c} + \mathbf{c_c})$ and the superspace group *Pm*(*s*) seem to lead to the most convincing displacive model. Indeed, this choice gives excellent agreement with the measurements, in particular with the satellites. This model is clearly the best one under the hypothesis of a purely displacive modulation and it provides a ferrielectric character for this phase. It should, however, be confirmed by the observation of main or satellite reflections in the incommensurate phase, even by weak ones.

No presentation of the numerous attempts to refine disordered models (modulated or of even more complex domain structure) is made in this article. Indeed, the strong correlation between population parameters and twin-volume ratios led invariably to unrealistic values for these parameters.

We have, thus, been able to identify the principal characteristics of the incommensurability in Pb_2CoWO_6. Two types of competing interactions seem to coexist. One of antiferroelectric type associated with an antiparallel shift of the Pb atoms, including possible frustrations with second nearest neighbors, the other of

Table 9. *Results of a refinement in Pm(s) for* $\mathbf{q}_{m4}$, *with ADP's for the* Pb *atoms*

Layers	All	$m = -1$	$m = 0$	$m = 1$
No. of reflections	3693	1000	1606	1087
OSR	0.9987	0.9942	1.0000	0.9973
R_w	0.0547	0.0865	0.0382	0.0903
R	0.0454	0.0733	0.0309	0.0814
	Pb_1	Pb_2	Pb_3	Pb_4
x_1	0.22761 (14)	0.25389 (20)	0.25804 (20)	0.22688 (16)
$a_{2,1}$	0.03572 (28)	−0.02285 (29)	0.01817 (38)	−0.03049 (28)
$b_{2,1}$	0.03154 (33)	−0.03202 (27)	−0.04268 (34)	−0.03098 (33)
x_3	0.00450 (17)	0.24020 (12)	0.50130 (17)	0.75717 (17)
β_{11}	0.00295 (12)	0.00284 (09)	0.00446 (12)	0.00416 (14)
β_{22}	0.00136 (18)	0.00278 (19)	0.01367 (43)	0.00136 (19)
β_{33}	0.00130 (05)	0.00161 (06)	0.00325 (08)	0.00177 (06)
β_{13}	−0.00026 (09)	−0.00100 (07)	−0.00073 (15)	−0.00028 (10)
	Pb_5	Pb_6	Pb_7	Pb_8
x_1	0.74521 (17)	0.73902 (18)	0.76827 (14)	0.76055 (16)
$a_{2,1}$	−0.03974 (35)	0.04171 (25)	0.04063 (31)	0.02243 (31)
$b_{2,1}$	−0.04585 (32)	−0.00441 (33)	−0.01648 (33)	0.03457 (28)
x_3	0.00656 (17)	0.23979 (12)	0.50521 (15)	0.76513 (12)
β_{11}	0.00165 (09)	0.00489 (15)	0.00306 (14)	0.00245 (11)
β_{22}	0.00468 (22)	0.00203 (23)	0.00890 (34)	0.00263 (20)
β_{33}	0.00178 (06)	0.00229 (08)	0.00298 (08)	0.00229 (08)
β_{13}	0.00126 (09)	−0.00123 (09)	−0.00064 (13)	0.00039 (09)

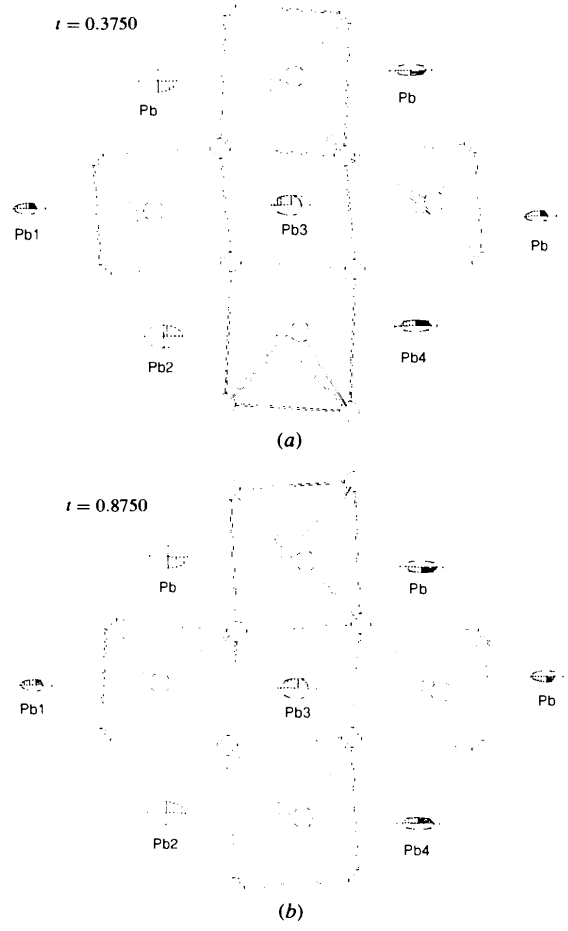

Fig. 5. Typical configurations, from the refinement based on *Pm(s)* and $\mathbf{q}_{m4}$, illustrating the evolution of the structure as a function of t.

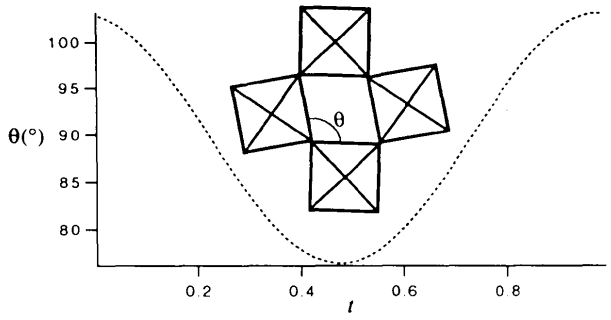

Fig. 6. Variation of the angle θ as a function of the internal coordinate t from the refinement in *Pm(s)* and $\mathbf{q}_{m4}$.

a more geometrical or sterical nature which corresponds to rotations and/or deformations of the oxygen octahedra in order to accommodate the displacements of the Pb atoms.

We would like to thank Professor H. Schmid and the members of his group for providing the crystal samples and for their continuous interest in the project. Financial support from the Swiss National Science Foundation is gratefully acknowledged.

References

ALEKSANDROV, K. & MISYUL, S. (1981). *Kristallografiya* **26**, 1074.

BALDINOZZI, G., SCIAU, PH. & BUFFAT, P. A. (1993). *Solid State Commun.* **86**, 541–544.

BALDINOZZI, G., SCIAU, PH. & LAPASSET, J. (1992). *Phys. Status Solidi A*, **133**, 17–23.

BLESSING, R. H. (1987). *Cryst. Rev.* **1**, 3–55.

BRIXEL, W., BOUTELLIER, R. & SCHMID, H. (1987). *J. Cryst. Growth*, **82**, 396-404.

BRIXEL, W., WERK, M. L., FISCHER, P., BÜHRER, W., RIVERA, J.-P., TISSOT, P. & SCHMID, H. (1985). *Jpn. J. Appl. Phys. Suppl.* **24**, 242–244.

BÜHRER, W., RÜDLINGER, M., MAAROUFI, F., TOLEDANO, P., SCHMID, H., BRIXEL, W. & SCIAU, PH. (1989). *Physica B*, **157**, 10–11.

FILIP'EV, V. S. & FESENKO, E. G. (1964). *Soviet Phys. Crystallogr.* **9**, 231–233.

JAMESON, G. B. (1982). *Acta Cryst.* A**38**, 817–820.

KIM, H.-J., LEE, B.-C. & CHOO, W.-K. (1992). *Ferroelectrics*, **125**, 233–238.

KIZHAEV, S. A. & BOKOV, V. A . (1966). *Fiz. Tverd. Tela*, **8**, 1554.

PACIOREK, W. A. (1991). *Methods of Structural Analysis of Modulated Structures and Quasicrystals*, edited by J. M. PÉREZ-MATO, F. J. ZÚÑIGA & G. MADARIAGA, pp. 268–279. Singapore: World Scientific.

PETŘÍČEK, V. & COPPENS, P. (1988). *Acta Cryst.* A**44**, 235–239.

RANDALL, C. A., MARKGRAF, S. A., BHALLA, A. S. & BABA-KISHI, K. (1989). *Phys. Rev. B*, **40**, 413–416.

SCIAU, PH., CALVARIN, G., SUN, B. N. & SCHMID, H. (1992). *Phys. Status Solidi A*, **129**, 309–321.

SCIAU, PH., KRUSCHE, K., BUFFAT, P. A. & SCHMID, H. (1990). *Ferroelectrics*, **107**, 235–240.

SUN, B. S., BOUTEILLER, R., SCIAU, PH., BURKHARDT, E., RODRIGUEZ, V. & SCHMID, H. (1991). *J. Cryst. Growth*, **112**, 71–83.

TAMURA, H. (1978). *Ferroelectrics*, **21**, 449–450.

WOLFF, P. M. DE, JANSSEN, T. & JANNER, A. (1981). *Acta Cryst.* A**37**, 625–636.